Title

Glucoraphanin and sulforaphane mitigate TNFα-induced Caco-2 monolayers permeabilization and inflammation.

Authors

Zhu, Wei

Cremonini, Eleonora

Mastaloudis, Angela

et al.

Publication Date

2024-10-01

DOI

10.1016/j.redox.2024.103359

Peer reviewed

Redox Biology 76 (2024) 103359

Contents lists available at ScienceDirect

Redox Biology

journal homepage: www.elsevier.com/locate/redox

Glucoraphanin and sulforaphane mitigate TNFα-induced Caco-2 monolayers permeabilization and inflammation

Wei Zhu [a], Eleonora Cremonini [a], Angela Mastaloudis [b], Patricia I. Oteiza [a,c,*]

[a] Department of Nutrition, University of California, Davis, CA, USA
[b] Brassica Protection Products LLC, Baltimore, MD, USA
[c] Department of Environmental Toxicology, University of California, Davis, CA, USA

ARTICLE INFO

Keywords:
Sulforaphane
Glucoraphanin
Intestinal barrier
Intestinal inflammation
Barrier permeabilization
Tumor necrosis factor alpha

ABSTRACT

Intestinal permeabilization is central to the pathophysiology of chronic gut inflammation. This study investigated the efficacy of glucoraphanin (GR), prevalent in cruciferous vegetables, particularly broccoli, and its derivative sulforaphane (SF), in inhibiting tumor necrosis factor alpha (TNFα)-induced Caco-2 cell monolayers inflammation and permeabilization through the regulation of redox-sensitive events. TNFα binding to its receptor led to a rapid increase in oxidant production and subsequent elevation in the mRNA levels of NOX1, NOX4, and Duox2. GR and SF dose-dependently mitigated both these short- and long-term alterations in redox homeostasis. Downstream, GR and SF inhibited the activation of the redox-sensitive signaling cascades NF-κB (p65 and IKK) and MAPK ERK1/2, which contribute to inflammation and barrier permeabilization. GR (1 μM) and SF (0.5–1 μM) prevented TNFα-induced monolayer permeabilization and the associated reduction in the levels of the tight junction (TJ) proteins occludin and ZO-1. Both GR and SF also mitigated TNFα-induced increased mRNA levels of the myosin light chain kinase, which promotes TJ opening. Molecular docking suggests that although GR is mostly not absorbed, it could interact with extracellular and membrane sites in NOX1. Inhibition of NOX1 activity by GR would mitigate TNFα receptor downstream signaling and associated events. These findings support the concept that not only SF, but also GR, could exert systemic health benefits by protecting the intestinal barrier against inflammation-induced permeabilization, in part by regulating redox-sensitive pathways. GR has heretofore not been viewed as a biologically active molecule, but rather, the benign precursor of highly active SF. The consumption of GR and/or SF-rich vegetables or supplements in the diet may offer a means to mitigate the detrimental consequences of intestinal permeabilization, not only in disease states but also in conditions characterized by chronic inflammation of dietary and lifestyle origin.

1. Introduction

Chronic gut inflammation, characterized by a dysregulated immune response and compromised barrier function, contributes to numerous gastrointestinal and systemic disorders [1–3]. The delicate homeostasis maintained by the intestinal barrier, crucial for efficient nutrient absorption and effective immune defense, can be disrupted under inflammatory conditions. Environmental factors, including dietary components, toxins, pathogens, stress, cytokines, obesity and other metabolic disorders could all lead to intestinal barrier disruption [4,5]. Tumor necrosis factor alpha (TNFα), a pro-inflammatory cytokine, is a major player in intestinal inflammatory processes, being known to compromise the integrity of the intestinal barrier. Barrier permeabilization can cause local and systemic inflammation, which can ultimately promote the development of several conditions and diseases, including endotoxemia, insulin resistance, metabolic syndrome, metabolic dysfunction-associated steatotic liver disease (MASLD, formerly known as NAFLD) type 2 diabetes, cardiovascular disease, and neuroinflammation [1–3,6]. Therefore, preserving the intestinal barrier function and lowering intestinal inflammation is essential to preserve intestinal and overall health.

The integrity and functionality of the intestinal barrier are regulated by the tight junctions (TJs), structures composed by membrane and cytosolic proteins including occludins, claudins, zonula occludens (ZOs), and junctional adhesion molecules [7]. TJs control the paracellular transport of water and ions and prevent the passage of luminal toxins

* Corresponding author. Departments of Nutrition and Environmental Toxicology, University of California, Davis, CA, USA.
E-mail address: poteiza@ucdavis.edu (P.I. Oteiza).

https://doi.org/10.1016/j.redox.2024.103359
Received 2 September 2024; Received in revised form 15 September 2024; Accepted 16 September 2024
Available online 17 September 2024

and pathogens [8]. Therefore, TJs play a crucial role in sustaining gut and systemic health. TNFα promotes the dysregulated opening of TJs and subsequent intestinal permeabilization through different mechanisms [9,10]. TNFα increases matrix metalloproteinase (MMP) 2 and 9 expression and/or activity which can degrade TJ proteins directly, leading to a disruption of barrier integrity [11,12]. Through the activation of nuclear factor κB (NF-κB) and extracellular regulated protein kinase 1/2 (ERK1/2), TNFα causes an increased phosphorylation of the myosin light chain (MLC) at Ser18/19 which leads to TJ opening. This can occur through the inhibition of the MLC phosphatase and/or an increased transcription of the MLC kinase (MLCK) that phosphorylates MLC [13,14]. Additionally, TNFα-mediated up-regulation of NADPH oxidases (NOX) activity and expression, and increased oxidant production [15], further activate redox sensitive signaling that promote inflammasome activation and the production and secretion of inflammatory interleukins [16]. Overall, the above sequence of events promotes intestinal permeabilization and sustained inflammation, contributing to the development of associated chronic conditions and diseases [17].

Diet has a major and direct impact on intestinal permeabilization and systemic health given that intestinal cells are directly exposed to high concentrations of dietary compounds [18,19]. Among the bioactives receiving attention for their health-promoting properties are glucoraphanin (GR) and its derivative sulforaphane (SF), primarily found in cruciferous vegetables such as broccoli [20] (Fig. 1A). Crucifer-rich diets have been linked to various health benefits, which have been attributed to SF, as GR has largely been considered to be biologically inert [21]. In the intestine, GR undergoes conversion to SF by the enzyme myrosinase, which is present in both plants and the intestinal microbiota, and SF is subsequently absorbed and metabolized to its bioactive metabolites including SF-glutathione (SF-GSH), SF-cysteine (SF-CYS), and SF-N-acetyl-L-cysteine (SF-NAC) through the mercapturic acid pathway in intestine and in liver. SF's health benefits are attributed to its capacity, and perhaps that of its metabolites' capacity to upregulate antioxidant defenses via Nrf2 activation [22], promoting anti-inflammatory [23] and anti-cancer [24] effects. On the other hand, its precursor GR is mostly non-absorbable and considered biologically inactive.

Supplementation with pure GR or GR-containing food has been shown to have beneficial metabolic effects, including improvement of lipid and glucose homeostasis [25–27]. Nevertheless, discerning whether the observed positive outcomes are directly attributable to GR is challenging, as the colon microbiota of mice and humans has the capability to hydrolyze GR into SF, though the conversion is limited and

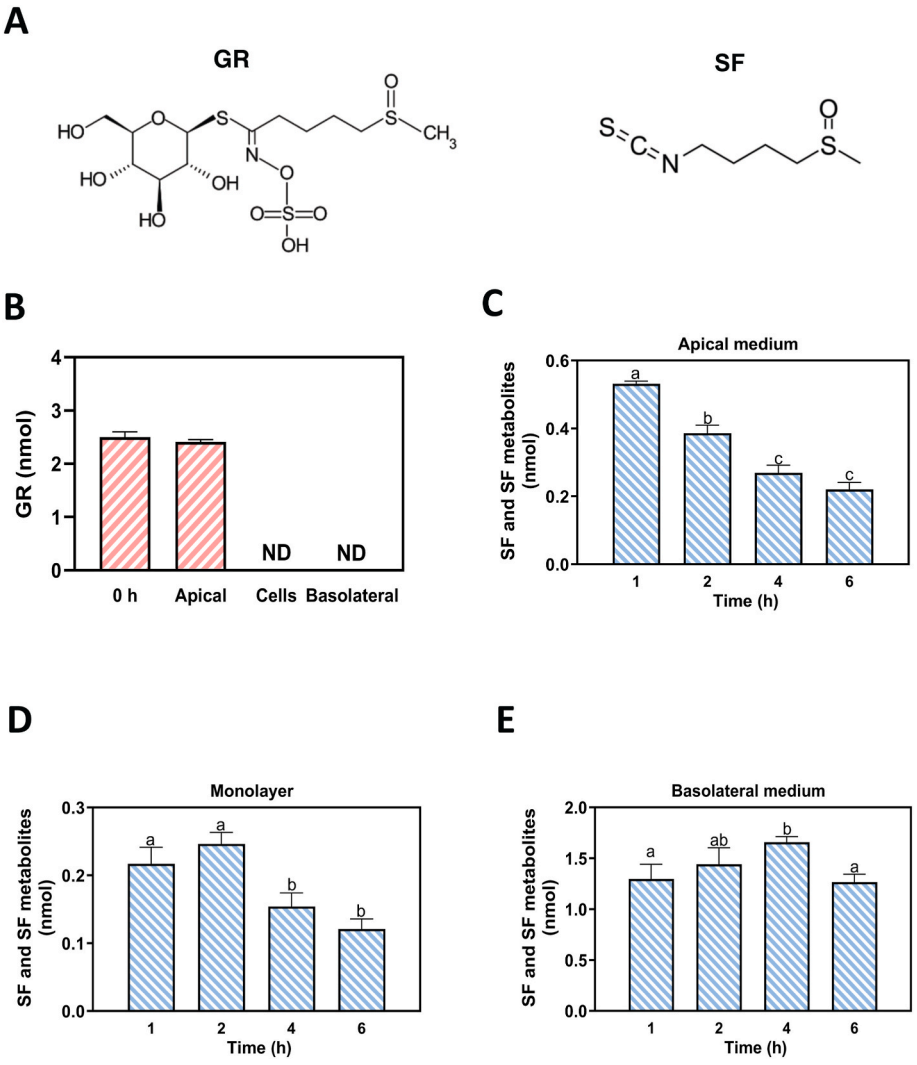

Fig. 1. Transport of GR and SF across Caco-2 cell monolayers. (**A**) Chemical structure of GR and SF. (**B-E**) Caco 2 cell monolayers, cultured in 6-well transwell inserts, were added to the apical compartment with 10 μM of (**B**) GR or (**C-E**) SF for 0–6 h. GR and SF concentrations were measured byUPLC-(ESI+)-MS/MS, as described in methods, at each time point in the apical and basiolateral medium and in the cell monolayers. Data are shown as mean ± SEM of 4 independent experiments. Values having different superscripts are significantly different (One-way ANOVA, $p < 0.05$). N.D.: Not detectable.

highly variable from person to person. Among the observed effects, a reduction in endotoxemia [28] could be mediated by local effects of GR at the gastrointestinal tract, protecting barrier function. Thus, this study investigated, using the well-established *in vitro* intestinal model of Caco-2 cell monolayer, to investigate the capacity of both GR and SF to mitigate TNFα-induced inflammation, TJs disruption and monolayer permeabilization. We investigated the underlying mechanisms, including the activation of redox-sensitive signaling pathways and events involved in the modulation of TJs structure and dynamics. We observed that, although with different potency, both GR and SF actively mitigated the cascades of events triggered by TNFα leading to monolayer permeabilization and sustained inflammation. While there is extensive research published on the potential health benefits of SF, to our knowledge, this is the first evidence supporting a beneficial health effect for GR. This novel concept will help to re-evaluate the intestinal and systemic health benefits of cruciferous vegetables.

2. Material and methods

2.1. Materials

GR and SF (purity >95.0 % by HPLC) were obtained from Cayman Chemical (Ann Arbor, MI). Caco-2 cells were from the American Type Culture Collection (Rockville, MA). Cell culture media MEM, 5-(and-6)-carboxy-2′, 7′-dichlorodihydrofluorescein diacetate (H2DCFDA, DCF as oxidized form), primary antibodies for ZO-1 (#33–9100), occludin (#33–1500) and claudin-1 (#71–7800) were from Invitrogen/Life Technologies (Grand Island, NY). Human interferon gamma (IFN-γ) and primary antibodies for phospho (Ser176/180)-IKKα/β (#2697), IKKα/β (#2370), phospho (Ser536)-p65 (#3033), p65 (#8242), phospho (Thr202/Tyr204)-ERK1/2 (#4370), ERK1/2 (#9102), β-actin (#12620) and secondary antibody goat anti-rabbit IgG (#7074) were from Cell Signaling Technology (Danvers, MA). IL-1β (#sc32294) was from Santa Cruz Technology (Santa Cruz, CA). IL-6 high-sensitive human ELISA kit was obtained from Abcam (Cambridge, UK), and human IL-8 DuoSet ELISA kit was obtained from R&D systems (Minneapolis, MN). The Millicell cell culture inserts and dihydroethidium (DHE) were from EMD Millipore (Hayward, CA). The Amplex Red Hydrogen Peroxide/Peroxidase Assay Kit was from ThermoFisher Scientific (Waltham, MA). Human TNFα, fluorescein isothiocyanate (FITC)-dextran, sulphorhodamine B (SRB), 3-[4,5-dimethylthiazol-2-yl]-2,5 diphenyl tetrazolium bromide (MTT), apocynin, VAS-2870, and DPI were from Sigma Aldrich (St Louis, MO). PVDF membranes and Clarity Western ECL Substrate were from Bio-Rad (Hercules, CA). The standards of GR, SF, SF-GSH, SF-CYS, and SF-NAC for UHPLC-ESI (+)-MS/MS analysis were from Toronto Research Chemical (Toronto, Canada). All LC-MS grade solvents were obtained from ThermoFisher Scientific (Waltham, MA).

2.2. Cell culture and incubation

Caco-2 cells between passages 5 to 20 were cultured at 37 °C in a 5 % (v/v) CO_2 atmosphere. Cells were grown and differentiated in MEM supplemented with 10 % (v/v) fetal bovine serum, antibiotics (50 U/ml penicillin and 50 μg/ml streptomycin), 1 % (v/v) of 100 × non-essential amino acids and 1 mM sodium pyruvate. For the experiments, Caco-2 cells were differentiated for 21 days in 24-well transwell inserts or 12 days in dishes. For the treatments, differentiated Caco-2 cells were firstly pre-incubated with IFN-γ (10 ng/ml) for 24 h in complete MEM media to upregulate the TNFα receptor. Subsequently, the medium was replaced by serum/phenol red-free MEM, cells were added without or with 0.1–1 μM of GR or SF for 30 min (added to the upper chamber when cells were differentiated in inserts), and subsequently incubated without or with TNFα (10 ng/ml) (added to the lower chamber when cells were differentiated in inserts) for 5 min up to 6 h, depending on the measurements. Proteins, mRNA and culture media were collected and processed accordingly, based on different determinations.

2.3. Determination of GR and SF transport across Caco-2 cell monolayers

Differentiated Caco-2 monolayers cultured on 6-well transwell inserts were treated with GR or SF of 10 μM for 0–6 h. Cells and apical and basolateral media were collected for GR, SF and SF metabolites analysis. GR, SF and SF metabolites were resolved chromatographically and quantified by UHPLC-ESI (+)-MS/MS using an UHPLC system coupled with a 6460 tandem mass spectrometer (Agilent Technologies, CA) according to our previously described procedure [29]. Poroshell 120 Bonus-RP column (2.1 × 150 mm, 2.7 μm) equipped with a Bonus-RP guard column (2.1 × 5 mm, 2.7 μm) (Agilent Technologies, CA) was used to separate the target compounds. Dynamic multiple reaction monitoring (MRM) was performed in positive ion mode to characterize and quantify the target compounds.

2.4. Transepithelial electrical resistance (TEER)

To measure Caco-2 monolayers permeability, TEER and FITC-dextran transport were measured in the 21-day differentiated Caco-2 monolayer cultured on 24-well transwell inserts (12 mm, 0.4 μm pore polyester membranes) at a seeding density of 3×10^4 cells. TEER was measured using a Millicell-ERS Resistance System that included a dual electrode-voltohm-meter (Millipore, Bedford, MA). To assess the impact of GR or SF on TEER, TEER values were first recorded after IFN-γ (10 ng/ml) incubation for 24 h. TEER values were measured again after GR or SF (0.1–1 μM) and TNFα (10 ng/ml) treatments for 6 h. TEER was calculated using the formula: $TEER = (R_m - R_i) \times A$, where R_m represents transmembrane resistance, R_i represents the intrinsic resistance of a cell-free medium, and A denotes the surface area of the membrane in cm^2. Arbitrary units (A. U.) were calculated based on TEER change for the control (non-added) monolayers.

2.5. FITC-dextran clearance

The paracellular transport through Caco-2 cell monolayers was determined by measuring the apical-to-basolateral clearance of FITC-dextran (4 kDa). Caco-2 monolayers differentiated on transwell inserts were treated as discussed for TEER determinations. After 6 h of incubation with TNFα, the medium was replaced in both compartments with fresh serum and phenol red-free MEM, FITC-dextran was then added to the apical compartment (100 μM final concentration). After 4 h incubation 100 μl of the medium in the basolateral compartment was collected and diluted with 100 μl 1X HBSS. The FITC fluorescence was measured at λex/λem = 485/530 nm in a Bio-Tek plate reader (Winooski, VT). The FITC-dextran clearance (CLFITC) was calculated using the equation $f_{FITC}/(F_{FITC}/A)$, where f_{FITC} is flux of FITC-dextran (in fluorescence units/h); F_{FITC}, the fluorescence of FITC-dextran in the upper compartment at zero time (in fluorescence units per nl); and A, the surface area of the membrane (1 cm^2). Arbitrary units (A.U.) were calculated based on the CL value for the non-added (control) cells (75 $nl/h/cm^2$).

2.6. Western blot

After the corresponding treatments, total proteins were isolated and quantified using the Bradford method as previously described [30]. Aliquots containing 30–50 μg protein were separated by 7–15 % (w/v) polyacrylamide gel electrophoresis and electroblotted to PVDF membranes. Dual standards (colored (Bio-Rad Laboratories, Hercules, CA) and biotinylated (Cell Signaling Technologies, Danvers, MA)) were run simultaneously. Membranes were blocked for 1 h in 5 % (w/v) non-fat milk in TBST buffer (50 mM Tris, 150 mM NaCl, pH = 7.6, 0.1 % (v/v) Tween-20), then incubated at 4 °C overnight with the corresponding antibodies (1:1000 dilution) in 1 % (w/v) bovine serum albumin in TBST buffer. After incubation for 1.5 h at room temperature with the secondary antibody (HRP-conjugated) (1:10,000 dilution), the

conjugates were visualized by chemiluminescence detection in a ChemiDoc Imaging Systems (Bio-Rad, Hercules, CA).

2.7. RNA isolation and qPCR

After the corresponding treatments, the RNA was extracted with TRIzol reagent (Invitrogen, Carlsbad, CA). cDNA was generated using high-capacity cDNA Reverse Transcriptase Kit (Applied Biosystems, Grand Island, NY). mRNA levels of NOX1, NOX4, Duox2, MLCK, IL-6, IL-8, IL-1β, NLRP3 and TNFα were assessed by qPCR (iCycler, Bio-Rad, Hercules, CA) using the primers listed in Supplementary Table S1. Relative mRNA levels were normalized to β-actin as the housekeeping gene and calculated using the $2^{-\Delta\Delta Ct}$ method [31].

2.8. Secreted IL-6 and IL-8 determinations

Caco-2 cells were treated with IFN-γ, GR or SF and TNFα as previously described. After 6 h incubation with or without TNFα addition, the incubation medium was collected and then centrifuged at 800×*g* for 10 min to remove dead cells and debris. 100 μl of medium was used to determine IL-6 and IL-8 concentrations by ELISA kits following the manufacturer's protocol. Absorbance was measured at 450 nm (Bio-Tek Instruments, Winooski, VT). The concentrations of IL-6 and IL-8 in the incubation medium were calculated using the respective standard curves.

2.9. Oxidant levels measurement

Cell oxidant levels were estimated using the probes H2DCFDA, DHE, and Amplex Red [32]. Caco-2 cells were seeded in white/clear bottom 96-well plates at a density of 5×10^4 cells/well. After differentiation, cells were treated with IFN-γ for 24 h and then with GR or SF or NOX inhibitors for 30 min and subsequently with TNFα. To evaluate DHE/H2DCFDA oxidation, following a 10-min exposure to TNFα, the medium was aspirated, and cells were treated with 20 μM DHE or 25 μM H2DCFDA in serum/phenol red-free MEM for 30 min at 37 °C. Subsequently, cells were rinsed twice with 1X HBSS, and fluorescence was measured at $\lambda_{ex}/\lambda_{em} = 495/525$ nm and 520/605 nm for DHE and DCF, respectively. H_2O_2 released into the medium was measured 3 h after TNFα addition using the Amplex Red Hydrogen Peroxide/Peroxidase Assay Kit following the manufacturer's instructions. To standardize the three determinations, fluorescence values were normalized to the protein content determined with SRB. Fluorescence and absorbance were measured using a Bio-Tek plate reader (Winooski, VT).

2.10. Molecular docking

NOX1 PDB file was generated by AlphaFold predicted model [33]. GR and SF PDB files were generated from PubChem (https://pubchem.ncbi.nlm.nih.gov). After converting the file format, structures were optimized by removal of water molecules, addition of hydrogens and minimization of energy. Docking was subsequently done by CB-DOCK [34], and all visualizations were conducted by VMD.

2.11. Statistical analysis

Results are shown as means ± SEM (n = 3–6). Data were analyzed by one-way analysis of variance (ANOVA) using GraphPad Prism 10.0 (GraphPad Software, San Diego, CA). Fisher least significance difference test was used to examine differences between group means. A p value < 0.05 was considered statistically significant.

3. Results

3.1. Absorption and metabolism of GR and SF in Caco-2 monolayers

Incubation of Caco-2 cells with concentrations of either GR or SF up to 100 μM had no significant impact on cell viability, as evaluated by MTT assay (Supplementary Fig. S1), confirming a lack of toxicity of either compound up to 100 μM. The absorption and metabolism of GR and SF (10 μM) in Caco-2 monolayers were analyzed using UHPLC-(ESI+)-MS/MS method as we previously described [29]. Results showed that GR was not detectable in either cells or the basolateral medium, and there was no significant decrease in GR concentration in the apical medium observed after 6 h incubation at 37 °C (Fig. 1B). A 6-h incubation at 37 °C in the absence of cells did not affect GR concentration (Supplementary Fig. S2A). This suggests that GR concentration remains stable at 37 °C within the initial 6 h of incubation in the Caco-2 cell model and that GR absorption in Caco-2 cells is not detected during this period of incubation at the concentration tested (10 μM). With SF, however, 6-h incubation at 37 °C without cells resulted in ~18% degradation (Supplementary Fig. S2B), highlighting the lability and reactivity of SF. Following 1, 2, 4, and 6 h of incubation with cells, SF, and its metabolites SF-CYS and SF-GSH were detected in cells and in apical and basolateral media, indicating that SF is absorbed and metabolized by Caco-2 cells (Supplementary Fig. S3). There was a decline in the concentration of SF in the apical medium over time (Fig. 1C). Within the monolayers, SF showed an initial increase at 1 h followed by a subsequent decrease (Fig. 1D), whereas the concentration in the basolateral medium exhibited an increase from 1 to 4 h (Fig. 1E). At 4 h, the SF and SF metabolites in cells and in basolateral medium accounted for over 70 % of the total SF. These findings confirm previous evidence that, while GR showed no detectable absorption at 10 μM in Caco-2 cells and poor (~5%) absorption in rats [35], SF is readily taken up, metabolized and transported out in Caco-2 monolayers.

3.2. GR and SF protect Caco-2 cell monolayers against TNFα-induced permeabilization

The permeabilization of Caco-2 monolayers was assessed by measuring TEER and FITC-dextran clearance. The protective effects of GR and SF were each evaluated at 0.1, 0.5 and 1 μM concentrations. Indicating monolayer permeabilization, TNFα caused a 35% reduction in TEER values and an 80% increase in FITC-dextran clearance (Fig. 2). While at 0.1 nor 0.5 μM concentration, GR did not exhibit protective effects, 1 μM GR fully protected the Caco-2 cell monolayer against TNFα-induced permeabilization (Fig. 2A–C). SF mediated a full protection of the barrier at 0.5 and 1 μM concentrations (Fig. 2B–D). Thus, both GR and SF can prevent Caco-2 monolayer permeabilization. Interestingly, despite being previously considered not biologically active given its lack of absorption, at physiologically achievable concentrations in the intestinal context (1 μM), GR showed a protective effect on Caco-2 monolayers permeabilization. This suggests that both GR and SF may exert barrier-protective and anti-inflammatory effects at the gastrointestinal tract.

3.3. GR and SF protect Caco-2 cell monolayers from TNFα-induced tight junction disruption

The integrity of the TJ in terms of their protein composition and distribution is essential for their function. Therefore, we next investigated the effects of TNFα, GR and SF on the levels of the TJ proteins ZO-1, occludin, and claudin-1 by Western blot. Following a 6-h incubation with TNFα, ZO-1, and occludin levels were significantly decreased (30% and 25%, respectively), compared to the control, while claudin-1 remained unaffected (Fig. 3). Pre-incubation with 1 μM GR effectively prevented TNFα-induced decrease in ZO-1 and occludin, whereas 0.1 μM GR showed no protective effect. 0.5 μM GR prevented TNFα-induced

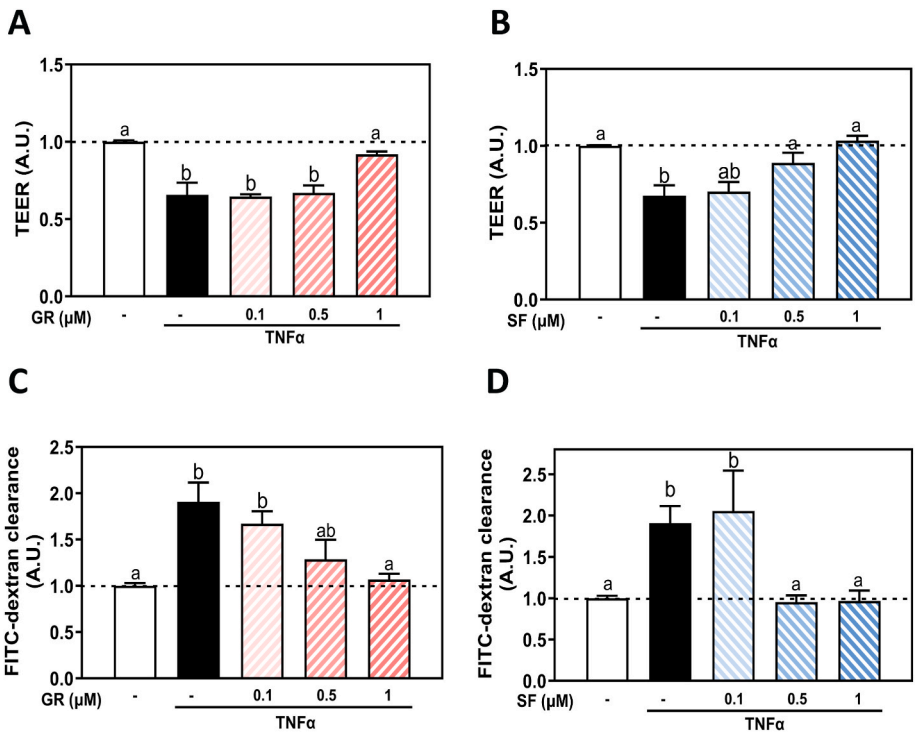

Fig. 2. Effects of GR and SF on TNFα-induced permeabilization of Caco-2 cell monolayers. Caco-2 cell monolayers, cultured in transwell inserts, were pre-incubated for 24 h with IFNγ (10 ng/ml) to upregulate the TNFα receptor. Then, 0.1–1 μM of GR or SF were added to the upper chamber and cells incubated for 30 min. TNFα (10 ng/ml) was subsequently added to the lower chamber and cells were incubated for an additional 6 h. Caco-2 cell monolayer permeability was evaluated by measuring: (**A, B**) TEER, and (**C, D**) FITC-dextran paracellular transport. Results are shown as mean ± SEM of 6 independent experiments. Values (A.U.: arbitrary units) were normalized to controls (1, dashed line). Values having different superscripts are significantly different ($p < 0.05$, One-way ANOVA).

decrease in ZO-1, not occludin (Fig. 3A). Preincubation with 0.5–1 μM SF fully prevented decreases in both ZO-1 and occludin (Fig. 3B). Neither GR nor SF had any impact on claudin-1 levels (Fig. 3C and D). This dose-dependency for GR and SF on TNFα-mediated TJ proteins decrease aligns with their protective effects on TEER and FITC-dextran clearance. Both GR and SF protect Caco-2 cell monolayers against TNFα-induced loss of TJ proteins.

3.4. GR and SF protect Caco-2 cell monolayers from TNFα-induced increased oxidant production

Considering the potential oxidative stress induced by pro-inflammatory stimuli, we next evaluated the effects of GR and SF on TNFα-mediated increased oxidant production using the probes H2DCFDA, DHE and Amplex red. After a 10-min incubation, TNFα resulted in a 22% increase in DCF fluorescence and a 20% increase in DHE fluorescence. Pre-incubation either with 1 μM GR or 0.1–1 μM SF fully prevented these increases in DCF (Fig. 4A). All tested concentrations of GR and SF were fully protective against DHE induced increases (Fig. 4B). The transient increase (10 min) in cellular oxidants was NOX-dependent, as evidenced by the inhibition of TNFα-mediated fluorescence increase by three well-known NOX inhibitors: apocynin, VAS-2870, and DPI, at 1 μM concentration. Hydrogen peroxide (H_2O_2) in the culture media was assessed using the Amplex Red/Peroxidase kit. Following a 3-h incubation, TNFα resulted in a 25% increase in media H_2O_2 concentration (Fig. 4C). This increase was completely prevented by 1 μM GR, 0.1–1 μM SF, and 1 μM NOX inhibitors.

Binding of ligands to proteins can significantly impact their function and activity. The transient (within 10 min of treatment with TNFα) O_2^- production is largely mediated by NOX1 activation. Since both GR and SF inhibited this production, we conducted molecular docking analysis to evaluate the potential binding of GR and SF to NOX1. NOX1, being a transmembrane protein, possesses several extracellular loops and six α-helix domains embedded within the cell membrane, with two heme groups located within the α-helix regions. Its NADPH catalytic site and co-enzyme FAD binding site are intracellularly situated (Fig. 4D). Since GR is mostly not absorbed by cells, including intestinal cells, we characterized the potential interaction of GR with the extracellular and transmembrane regions of NOX1 (Fig. 4E). Analysis of the involved amino acids residues in the transmembrane regions, suggested that GR could interact with NOX1 residues including Ser269, Asn61, Arg54, His265, Lys32, Tyr33, His115, His221 and Ala57 by both hydrogen bonds and hydrophobic interactions (Fig. 4F, Supplementary Fig. S4A). Of these residues, at a minimum, residues His115 and His221 are necessary in the interaction between the NOX1 protein and the heme group that is required for the electron transfer chain (Supplementary Fig. S4B), similar to the role of His115 and His222 in NOX2 [36]. The binding free energy of GR to the transmembrane regions of NOX1 is −6.7 kJ/mol. Since SF is rapidly absorbed by cells, we assessed the interactions of SF with the intracellular NOX1 region and determined that SF has potential binding capability to the outer heme group (Supplementary Fig. S4C) and also with the intracellular FAD binding site (data not shown).

Considering that NOX1, NOX4 and Duox2 are the predominant NOXs in intestinal cells [37,38], TNFα-induced O_2^-/H_2O_2 production could be also associated with the overexpression of these NOX genes. Thus, we next measured NOX1, NOX4, and Duox2 mRNA levels by qPCR. After a 6-h (NOX1) and 3-h (NOX4 and Duox2) incubation, TNFα induced 1.9-, 1.8- and 1.6-fold increases in NOX1, NOX4 and Duox2 mRNA levels, respectively. 1 μM GR and both 0.5–1 μM SF concentrations prevented these increases (Fig. 5A–F).

3.5. GR and SF protect Caco-2 cell monolayers from TNFα-induced activation of signaling pathways involved in TJ opening

The redox-sensitive NF-κB pathway is a crucial signaling pathway

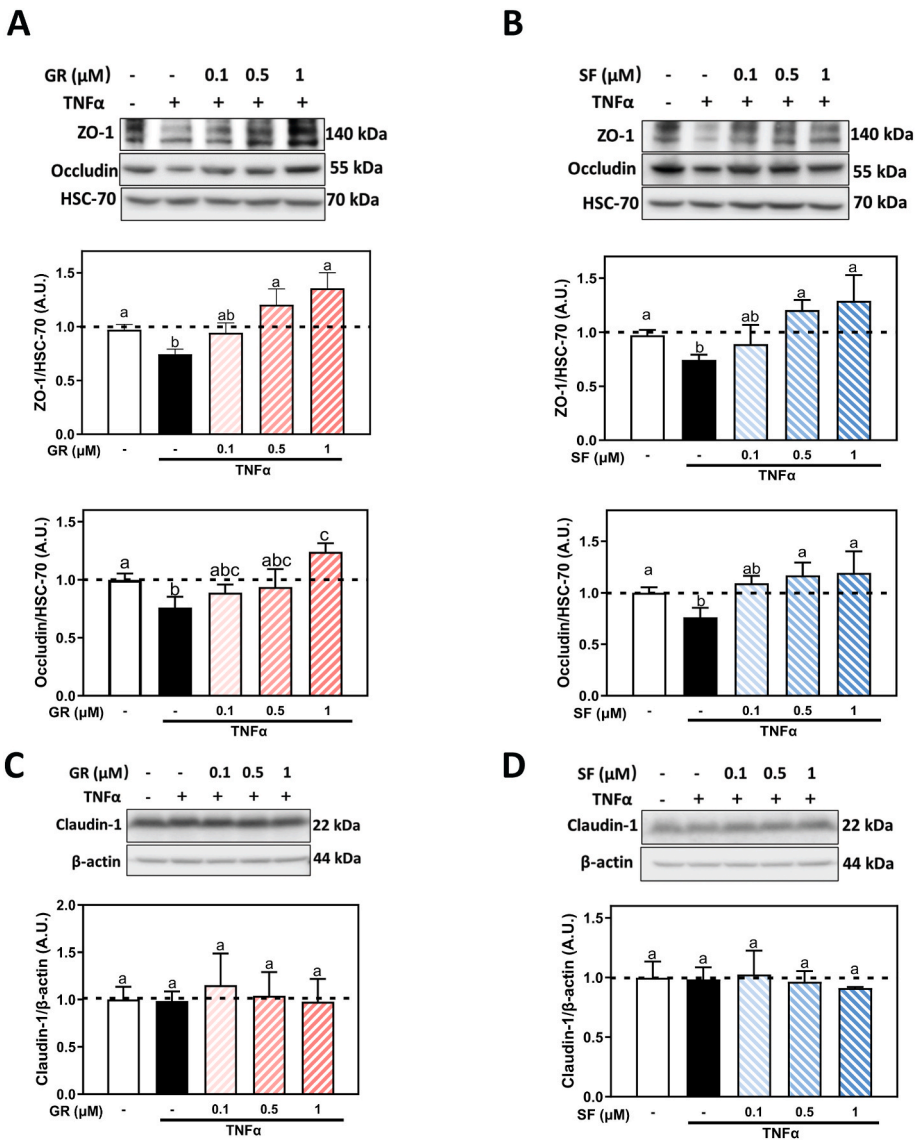

Fig. 3. Effects of GR and SF on TNFα-induced alterations in TJ proteins levels. (**A-F**) Caco-2 cell monolayers cultured in dishes were pre-incubated for 24 h with IFN-γ (10 ng/ml) to upregulate the TNFα receptor. Cells were then incubated without or with 0.1–1 μM (**A, C**) GR or (**B, D**) SF for 30 min, and subsequently without or with TNFα (10 ng/ml) for 6 h. ZO-1, occludin, and claudin-1 proteins levels were evaluated by Western blot. Bands were quantified and values referred to HSC-70 or β-actin levels (loading control). Results are shown as mean ± SEM of 4–6 independent experiments. Values having different superscripts are significantly different ($p < 0.05$, One-way ANOVA).

that regulates intestinal inflammation and barrier permeability. After a 5-min incubation, TNFα significantly increased IKK and p65 phosphorylation at Ser160/180 and Ser536, respectively, by approximately 30%. These increases were prevented by 1 μM GR and SF (Fig. 6A–D). Another pivotal pathway involved in intestinal inflammation and barrier permeabilization in response to proinflammatory stimuli is the ERK1/2 pathway. TNFα significantly increased ERK phosphorylation at Thr202/Tyr204 by 2.5 times after a 3-h incubation, which was prevented by 0.1–1 μM GR and SF. NF-κB and ERK1/2 regulate the expression of myosin light chain kinase (MLCK) [10,39], a central regulator of TJ opening [40]. TNFα caused a 50% increase in MLCK mRNA levels that was prevented by 0.5–1 μM GR and 0.1–1 μM SF (Fig. 6G and H).

3.6. GR and SF protect Caco-2 cell monolayers from TNFα-induced proinflammatory cytokine production

Through the activaton of NF-κB and MAPKs, TNFα promotes cytokine production and release. After a 6-h incubation period, TNFα caused a 1.7-fold increase in IL-6 mRNA levels and a 2.5-fold increase in IL-8 mRNA levels. GR and SF did not mitigate these increases in IL-6 or IL-8 mRNA levels in the range of concentrations tested (Fig. 7A–D). TNFα caused a 2.8-fold increase in TNFα mRNA level. While GR had no effect, SF at 1 μM concentration prevented-TNFα-mediated TNFα mRNA increase (Fig. 7E and F).

IL-6 and IL-8 secreted to the medium was measured by ELISA. TNFα caused 2.5-fold and 2.6-fold increases in IL-6 and IL-8 protein levels, respectively, in the cell culture medium. GR did not mitigate these increases in the range of concentrations tested. SF did not prevent the increase in IL-6 protein levels at 0.1–1 μM concentration, but was partially protective of the TNFα-induced IL-8 protein level increase at 0.5 and 1 μM (Fig. 7G–J).

3.7. GR and SF protect Caco-2 cell monolayers from TNFα-induced inflammasome activation

Following a 6-h incubation with TNFα, NLRP3, and IL-1β mRNA

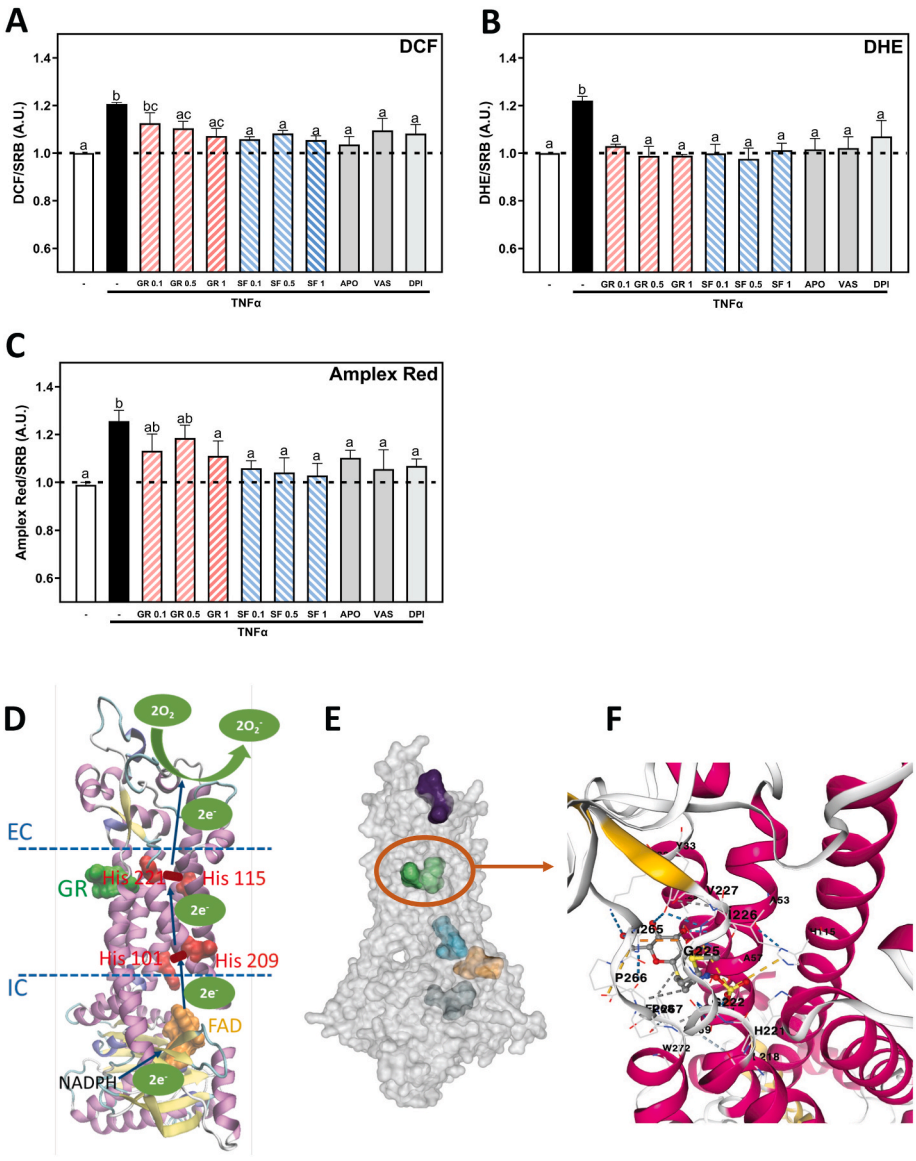

Fig. 4. GR and SF inhibit TNFα-induced oxidant production and potential interactions with NOX1. Caco-2 cell monolayers cultured in dishes were pre-incubated for 24 h with IFN-γ (10 ng/ml) to upregulate the TNFα receptor. Cells were then incubated without or with 0.1–1 μM GR, 0.1–1 μM SF and 1 μM Apo, VAS and DPI for 30 min, and subsequently without or with TNFα (10 ng/ml) for further 10 min (H2DCFDA, DHE) or 1 h (Amplex Red/Peroxidase). Cell oxidant levels were assessed using the probes (**A**) DCF and (**B**) DHE. (**C**) H_2O_2 release was measured in the medium using the Amplex Red/Peroxidase assay as described in Methods. All values were normalized to the protein content measures with SRB. Results are shown as mean ± SEM of 4–6 independent experiments. Data were normalized to control values. Values having different superscripts are significantly different ($p < 0.05$, one-way ANOVA). (**D**) Conformation and electrons transfer of NOX1. (**E, F**) Molecular modeling of the potential interactions of GR with NOX1. (For interpretation of the references to color in this figure legend, the reader is referred to the Web version of this article.)

levels increased 3.8 and 1.7-fold, respectively. These increases were mitigated by SF (1 μM), but no by GR (0.1–1 μM) (Fig. 8A–D). TNFα also caused a 70 % increase in cellular total IL-1β protein levels, which was prevented by 0.1–1 μM SF and by 1 μM GR (Fig. 8E and F).

4. Discussion

Intestinal inflammation is associated with increased intestinal permeability, which in turn is influenced by a range of factors including diet, stress, metabolic disorders, infections, autoimmune disorders, and inflammatory bowel diseases [41–43]. To date, SF has been attributed all of the health benefits linked to GR consumption. The present study demonstrated that, at concentrations attainable in the intestinal lumen from cruciferous vegetable consumption, not only SF but also GR exerted protective effects against TNFα-induced intestinal permeabilization and inflammation in Caco-2 monolayers, despite the fact that GR was not being taken up by the cells. This protection was achieved mainly through the regulation of oxidant production, activation of redox-sensitive signals and preservation of TJ structure. Considering that intestinal permeabilization causes metabolic endotoxemia, which underlies systemic inflammation leading to the development/progression of multiple chronic conditions including insulin resistance, GR protective actions at the intestinal level can in part contribute to the health benefits of cruciferous vegetables, which were previously attributed only to its metabolite, SF.

The binding of TNFα to its receptor is associated with a NOX-mediated transient increase in $O_2^{\cdot-}$ production, which in enterocytes is primarily due to NOX1 activation [44]. Transient cellular increases in $O_2^{\cdot-}$ and H_2O_2 levels are important for the enhancement of the cascade of events downstream of the binding of TNFα to its receptor, which is very

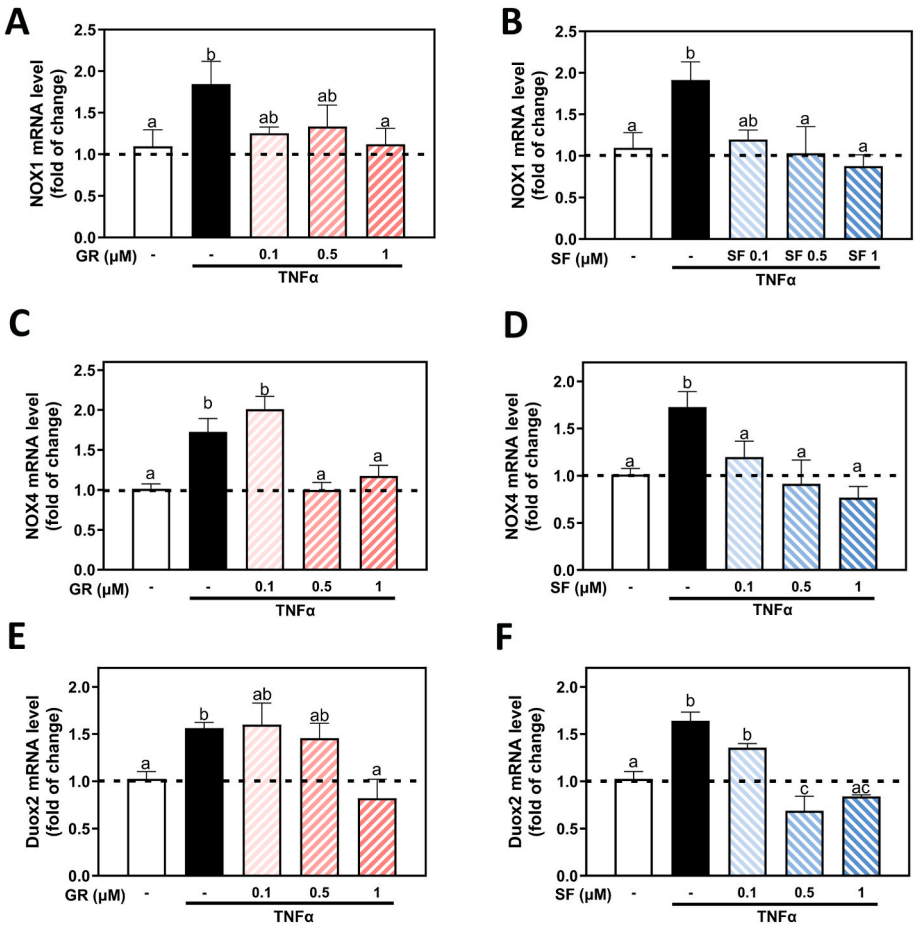

Fig. 5. Effects of GR and SF on TNFα-mediated increased expression of NOX1, NOX4 and Duox2. Caco-2 cell monolayers cultured in dishes were pre-incubated for 24 h with IFN-γ (10 ng/ml) to upregulate the TNFα receptor. Cells were then incubated without or with 0.1–1 μM GR or SF for 30 min, and subsequently without or with TNFα (10 ng/ml) for 6 h (NOX1) or 3 h (NOX4 and Duox2). **(A, B)** NOX1, **(C, D)** NOX4, and **(E, F)** Duox2 mRNA levels were determined by qPCR. The relative gene expression was normalized to β-actin as housekeeping gene. Results are shown as mean ± SEM of 4–6 independent experiments. Data were normalized to control values. Values having different superscripts are significantly different ($p < 0.05$, one-way ANOVA).

important for a physiological inflammatory response. However, high levels of TNFα in a chronic inflammatory condition can lead to a prolonged activation of NF-κB and ERK1/2, upregulation of NOX1 and NOX4, mitochondrial dysfunction and oxidative stress [15,45–48]. Molecular docking showed that GR could bind to the extracellular and transmembrane regions of NOX1, potentially inhibiting its activity. Such an inhibitory effect could explain why, even when GR is not absorbed, it could inhibit the TNFα-triggered cascade by decreasing the $O_2^{\cdot}/H_2O_2$ pulses that enhance the downstream cascade which ultimately leads to barrier permeabilization and inflammation. While this could be one explanation for the observed GR effects, other mechanisms including GR interactions with the TNFα receptor and/or with membrane lipid rafts cannot be excluded.

TNFα is a key mediator of intestinal inflammation [49] and barrier permeabilization [50]. Both processes involve TNFα-mediated activation of the redox-sensitive signals NF-κB and ERK1/2, that promote the production of proinflammatory cytokines and regulate events leading to TJ opening [39,50]. Additionally, TNFα causes decreases in the levels of the central TJ proteins ZO-1 and occludin, which could be related to alterations in their transcription/translation and/or to their degradation by metalloproteases. In fact, MMP-9 expression is upregulated by both NF-κB and ERK1/2 [51]. In terms of the regulation of barrier dynamics, NF-κB and ERK1/2 promote an increased transcription of MLCK, the kinase that phosphorylates MLC leading to the contraction of the actomyosin ring, TJ opening and enhanced barrier permeability [39,52,53]. In this scenario, ERK1/2 also contributes to deactivating the MLC phosphatase, leading to increased MLC phosphorylation levels [54,55]. Additionally, NF-κB is central to the upregulation of proinflammatory cytokines, including IL-6, IL-8, IL-β and TNFα [56] that would further contribute to the permeabilization of the barrier and the chronicity of the inflammatory process. Thus, the capacity of GR and SF to inhibit TNFα-mediated NF-κB and ERK1/2 activation explains their capacity to mitigate the associated Caco-2 cell monolayer permeabilization and increased cytokine production.

SF is the most well studied naturally occurring inducers of Nrf2 and it has been demonstrated to contribute to deliver major benefits to human health, whether delivered directly as SF or as its precursor GR, even at normal dietary levels [57]. Nonetheless, interest in GR and GR-rich vegetables so far has only been based on its bio-conversion to its hydrolysis product SF, given that GR does not have a known biological activity. Dietary GR is indeed very poorly absorbed (<5 % in a rodent model) [35]. In the present study, at 10 μM GR concentration in the apical medium, we did not observe detectable GR levels in cells or in the basolateral medium in Caco-2 monolayers, which further supports the concept that GR is poorly, if at all, absorbed by intestinal cells. Due to its direct poor bioavailibility and unknown biological activity, to our knowledge there has been no research conducted to specifically address GR biological effects. Cruciferous vegetables are commonly eaten cooked, exposing individuals to intact GR rather than to its hydrolysis product SF, given that cooking destroys myrosinase, the enzyme that catalyzes the conversion of GR into SF. GR hydrolysis can also occur in the lower gut, as the result of myrosinase activity present in the

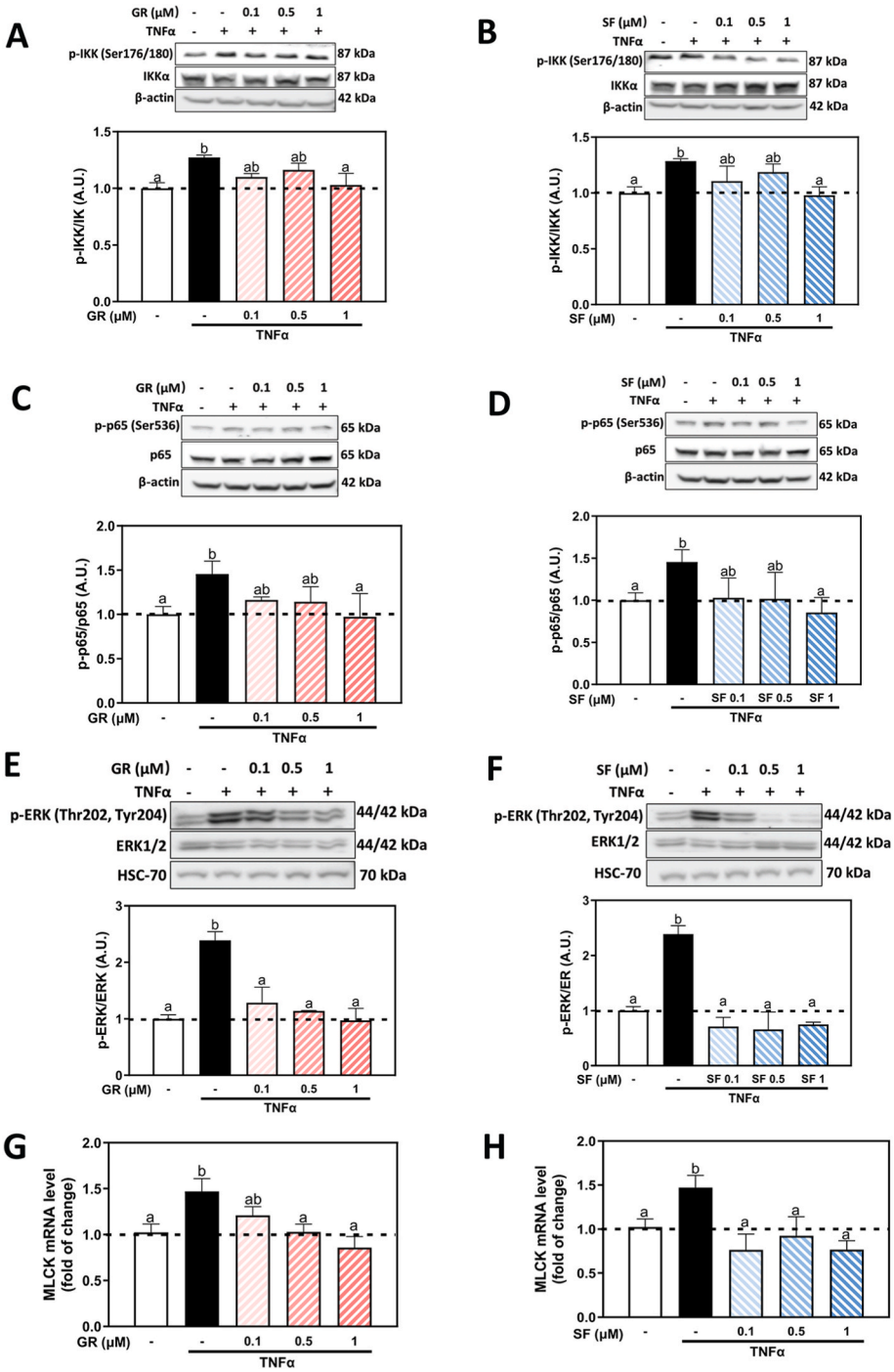

Fig. 6. Effects of GR and SF on TNFα-mediated NF-κB and ERK1/2 activation and increased MLCK gene expression. Caco-2 cell monolayers cultured in dishes were pre-incubated for 24 h with IFN-γ (10 ng/ml) to upregulate the TNFα receptor. Cells were then incubated without or with 0.1–1 μM GR or SF for 30 min, and subsequently without or with TNFα (10 ng/ml) for 5 min (for IKK and p65 phosphorylation) or 3 h (for ERK1/2 phosphorylation and MLCK mRNA level). (**A, B**) Total and phosphorylated IKK (Ser178/180), and (**C, D**) total and phosphorylated p65 (Ser536), and (**E, F**) total and phosphorylated ERK1/2 (Thr202/Tyr204) were measured by Western blot. β-actin was also determined as loading control. Western blot bands were quantified, and results are shown as mean ± SEM of 4–6 independent experiments. (**G, H**) MLCK mRNA levels were determined by qPCR. The relative gene expression was normalized to β-actin as housekeeping gene. Values having different superscripts are significantly different ($p < 0.05$, One-way ANOVA).

microbiota [58–60]. However, this conversion is very limited (~10 % of ingested GR) and highly variable (1–40 %). Given the above, research emphasis has focused on increasing GR conversion to SF in the small intestine by the addition of exogenous plant myrosinase, rather than in the understanding of potential direct biological effects of GR.

Many dietary components, including fiber, proanthocyanidins (polymerization degree> 4) have been shown to promote health benefits even when not absorbed at all or not absorbed as parent compounds [61, 62]. Their capacity to promote health is associated with their action at the gastrointestinal level, which results in systemic effects. In particular, sustaining the intestinal barrier function is critical to prevent the passage of unwanted luminal elements, i.e. pathogens, bacterial and food toxins, into the circulation. Thus, the paracellular transport of bacterial lipopolisaccharides and associated endotoxemia causes a condition of

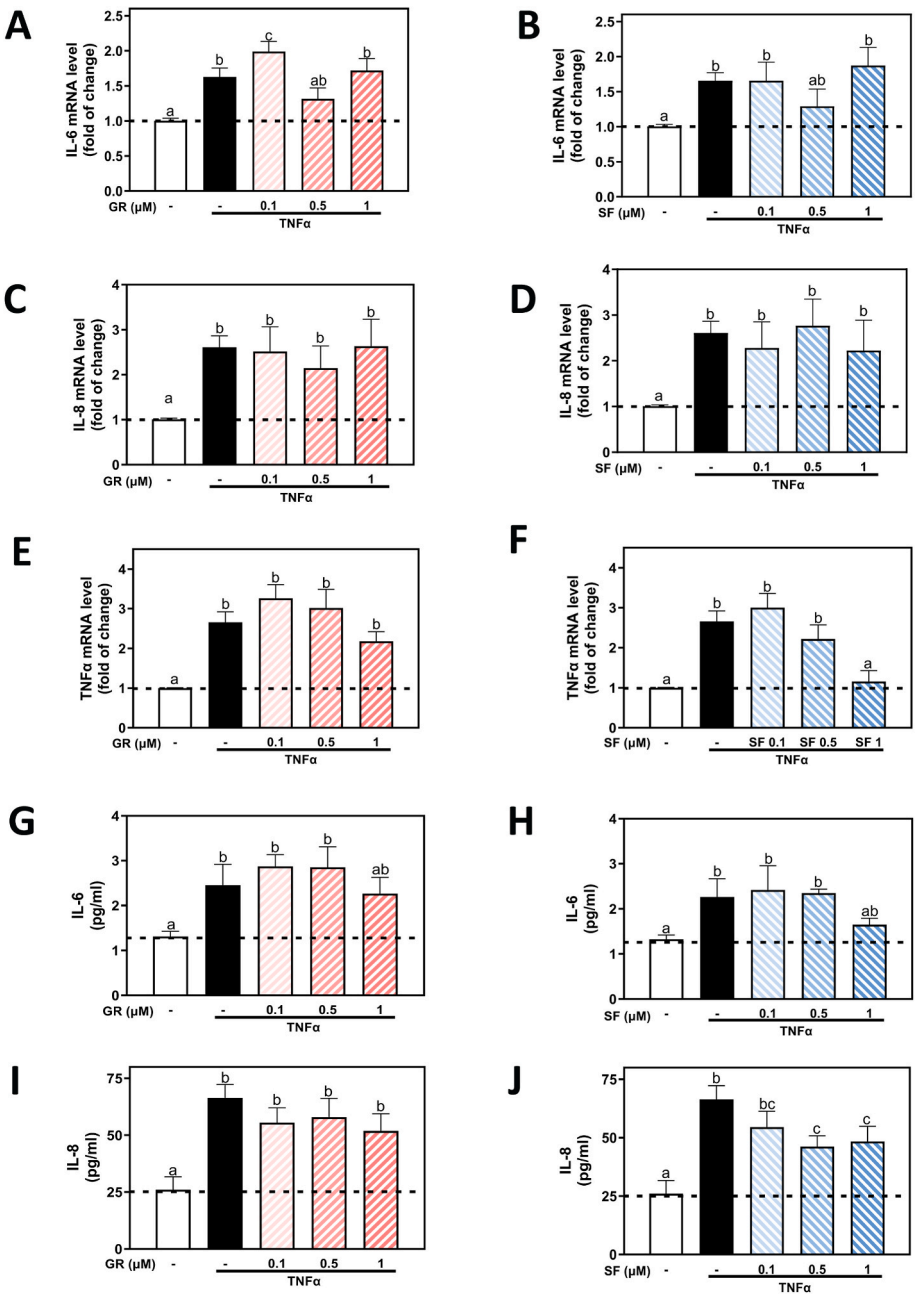

Fig. 7. Effects of GR and SF on TNFα-mediated increased expression and secretion of proinflammatory cytokines: IL-6, IL-8 and TNFα. Caco-2 cell monolayers cultured in dishes were pre-incubated for 24 h with IFN-γ (10 ng/ml) to upregulate the TNFα receptor. Cells were then incubated without or with 0.1–1 μM GR or SF for 30 min, and subsequently without or with TNFα (10 ng/ml) for 6 h. (**A, B**) IL-6 and (**C, D**) IL-8 (**E, F**) TNFα mRNA levels were determined by qPCR. The relative gene expression was normalized to β-actin as housekeeping gene. (**G, H**) IL-6, and (**I, J**) IL-8 released to the medium were measured by ELISA as described in Methods. Results are shown as mean ± SEM of 4–6 independent experiments. Values having different superscripts are significantly different ($p < 0.05$, one-way ANOVA).

chronic inflammation that is proposed to underlie several diseases, including obesity-associated type 2 diabetes, steatosis and neuroinflammation [63]. Thus, our observation of the capacity of GR to preserve intestinal barrier function can in part explain some of the health benefits previously only attributed to SF. In support of this, administration of 0.3 % (w/w diet) GR as boiled broccoli sprouts powder mitigated obesity-induced endotoxemia and associated insulin resistance and altered metabolic parameters [28]. Other beneficial actions observed for GR and GR-containing foods could be in part due to GR effects at the intestinal mucosa. They include the mitigation of dyslipidemia in high-fat diet-fed mice [25] and a reduction in plasma LDL cholesterol in humans [64]. However, discerning whether the health benefits described for SF, can be in part also attributed to GR is challenging, as the colon microbiota of mice and humans have the capability to hydrolyze GR into SF to a limited and variable degree.

To our knowledge, the present study is the first to demonstrate that not only SF but also GR can exert health benefits. Both, SF and GR mitigated TNFα-induced permeabilization and inflammation in Caco-2 cell monolayers. This effect is in part due to their capacity to inhibit TNFα-mediated NOX1 activation, increases in O_2/H_2O_2 production and NF-κB and ERK1/2 activation. Given the relevance of the gastrointestinal tract on overall health, the protection of barrier function is critical to prevent the pathologies associated to endotoxemia and its associated systemic inflammation.

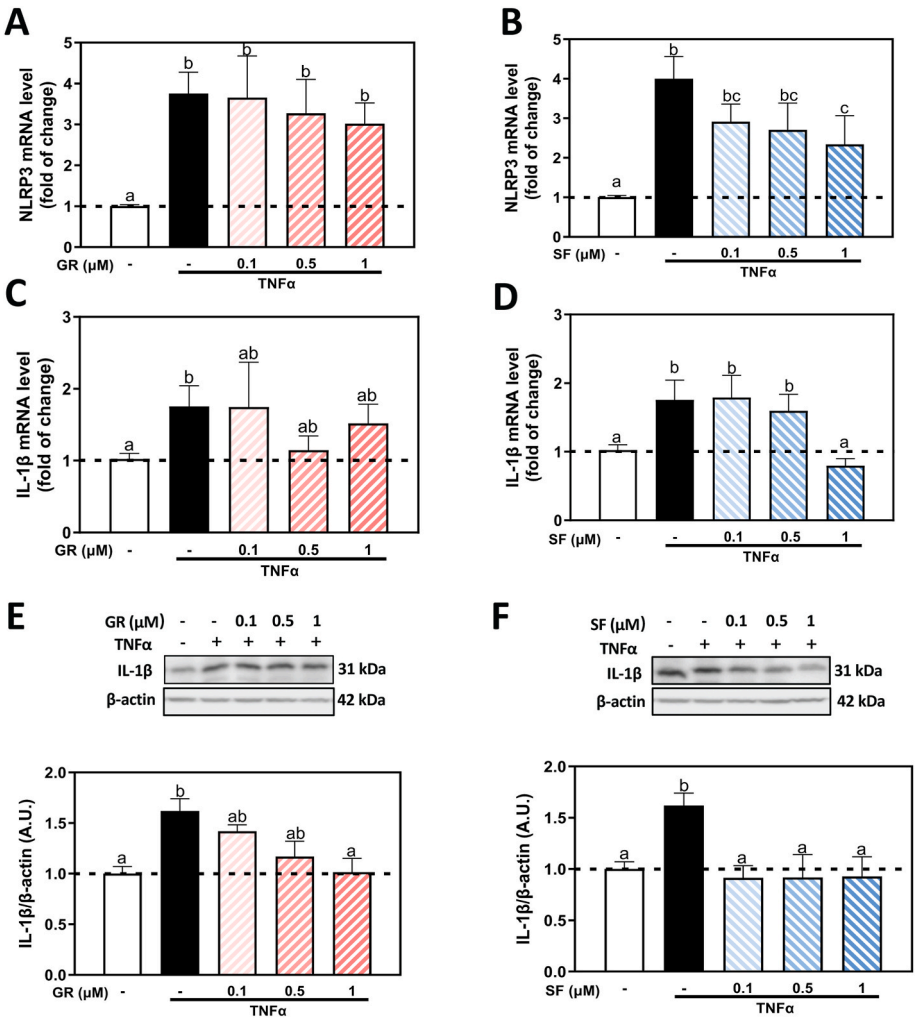

Fig. 8. Effects of GR and SF on TNFα-mediated activation of the inflammasome and increased expression of IL-1β. Caco-2 cell monolayers cultured in dishes were pre-incubated for 24 h with IFN-γ (10 ng/ml) to upregulate the TNFα receptor. Cells were then incubated without or with 0.1–1 μM GR or SF for 30 min, and subsequently without or with TNFα (10 ng/ml) for 6 h. (**A, B**) NLRP3 and (**C D**) IL-1β mRNA levels were determined by qPCR. The relative gene expression was normalized to β-actin as housekeeping gene. (**E, F**) Cellular total IL-1β and β-actin (loading control) were measured by Western blot. Results are shown as mean ± SEM of 4–6 independent experiments. Values having different superscripts are significantly different ($p < 0.05$, one-way ANOVA).

CRediT authorship contribution statement

Wei Zhu: Writing – original draft, Validation, Software, Methodology, Investigation, Formal analysis, Data curation, Conceptualization. **Eleonora Cremonini:** Writing – review & editing, Investigation, Formal analysis, Data curation, Conceptualization. **Angela Mastaloudis:** Writing – review & editing, Funding acquisition, Conceptualization. **Patricia I. Oteiza:** Writing – review & editing, Supervision, Conceptualization.

Declaration of competing interest

Authors have no conflict of interest to declare.

Data availability

Data will be made available on request.

Acknowledgement

This work was supported by funding from Brassica Protection Products LLC to E.C. and P. I. O., and grant NIFA-USDA (CA-D-NTR-2819-H) to P. I. O.

Appendix ASupplementary data

Supplementary data to this article can be found online at https://doi.org/10.1016/j.redox.2024.103359.

References

[1] N. Di Tommaso, A. Gasbarrini, F.R. Ponziani, Intestinal barrier in human health and disease, Int. J. Mol. Sci. 18 (23) (2021) 12836, https://doi.org/10.3390/ijerph182312836.
[2] J. Martel, et al., Gut barrier disruption and chronic disease, Trends Endocrinol. Metabol. 33 (4) (2022) 247–265, https://doi.org/10.1016/j.tem.2022.01.002.
[3] Y. Fouad, Metabolic-associated fatty liver disease: new nomenclature and approach with hot debate, World J. Hepatol. 15 (2) (2023) 123, https://doi.org/10.3748/wjg.v29.i3.549.
[4] A. Kosińska, W. Andlauer, Modulation of tight junction integrity by food components, Food Res. Int. 54 (1) (2013) 951–960, https://doi.org/10.1016/j.foodres.2012.12.038.
[5] D. Ulluwishewa, et al., Regulation of tight junction permeability by intestinal bacteria and dietary components, J. Nutr. 141 (5) (2011) 769–776, https://doi.org/10.3945/jn.110.135657.
[6] J.R. Turner, Intestinal mucosal barrier function in health and disease, Nat. Rev. Immunol. 9 (11) (2009) 799–809, https://doi.org/10.1038/nri2653.
[7] T. Suzuki, Regulation of intestinal epithelial permeability by tight junctions, Cell. Mol. Life Sci. 70 (4) (2013) 631–659, https://doi.org/10.1007/s00018-012-1070-x.

[8] M.A. Odenwald, J.R. Turner, The intestinal epithelial barrier: a therapeutic target? Nat. Rev. Gastroenterol. Hepatol. 14 (1) (2017) 9–21, https://doi.org/10.1038/nrgastro.2016.169.

[9] C. Chelakkot, J. Ghim, S.H. Ryu, Mechanisms regulating intestinal barrier integrity and its pathological implications, Exp. Mol. Med. 50 (8) (2018) 1–9, https://doi.org/10.1038/s12276-018-0126-x.

[10] D. Ye, I. Ma, T.Y. Ma, Molecular mechanism of tumor necrosis factor-α modulation of intestinal epithelial tight junction barrier, Am. J. Physiol. Gastrointest. Liver Physiol. 290 (3) (2006) G496–G504, https://doi.org/10.1152/ajpgi.00318.2005.

[11] Z. Abdullah, U. Bayraktutan, Suppression of PKC-α attenuates TNF-α-evoked cerebral barrier breakdown via regulations of MMP-2 and plasminogen–plasmin system, Biochim. Biophys. Acta (BBA) - Mol. Basis Dis. 1862 (7) (2016) 1354–1366, https://doi.org/10.1016/j.bbadis.2016.03.014.

[12] A. Al-Roub, et al., TNFα induces matrix metalloproteinase-9 expression in monocytic cells through ACSL1/JNK/ERK/NF-kB signaling pathways, Sci. Rep. 13 (1) (2023) 14351, https://doi.org/10.1038/s41598-023-41514-6.

[13] F. Wang, et al., Interferon-γ and tumor necrosis factor-α synergize to induce intestinal epithelial barrier dysfunction by up-regulating myosin light chain kinase expression, Am. J. Pathol. 166 (2) (2005) 409–419, https://doi.org/10.1016/S0002-9440(10)62264-X.

[14] W.V. Graham, et al., Tumor necrosis factor-induced long myosin light chain kinase transcription is regulated by differentiation-dependent signaling events: characterization of the human long myosin light chain kinase promoter, J. Biol. Chem. 281 (36) (2006) 26205–26215, https://doi.org/10.1074/jbc.M602164200.

[15] D.E. Iglesias, et al., Ellagic acid protects Caco-2 cell monolayers against inflammation-induced permeabilization, Free Radic. Biol. Med. 152 (2020) 776–786, https://doi.org/10.1016/j.freeradbiomed.2020.01.022.

[16] A.H. Chan, K. Schroder, Inflammasome signaling and regulation of interleukin-1 family cytokines, J. Exp. Med. 217 (1) (2019), https://doi.org/10.1084/jem.20190314.

[17] G.Y. Chen, G. Núñez, Inflammasomes in intestinal inflammation and cancer, Gastroenterology 141 (6) (2011) 1986–1999, https://doi.org/10.1053/j.gastro.2011.10.002.

[18] B. Lee, K.M. Moon, C.Y. Kim, Tight junction in the intestinal epithelium: its association with diseases and regulation by phytochemicals, Int. J. Immunol. Res. 2018 (2018) 2645465, https://doi.org/10.1155/2018/2645465.

[19] T. Suzuki, Regulation of the intestinal barrier by nutrients: the role of tight junctions, Anim. Sci. J. 91 (1) (2020) e13357, https://doi.org/10.1111/asj.13357.

[20] M.A. Prieto, C.J. López, J. Simal-Gandara, Chapter Six - glucosinolates: Molecular structure, breakdown, genetic, bioavailability, properties and healthy and adverse effects, in: I.C.F.R. Ferreira, L. Barros (Eds.), Adv. Food Nutr. Res., Academic Press, 2019, pp. 305–350.

[21] A.I. Amjad, et al., Broccoli-derived sulforaphane and chemoprevention of prostate cancer: from bench to bedside, Curr. Pharmacol. Rep. 1 (6) (2015) 382–390, https://doi.org/10.1007/s40495-015-0034-x.

[22] E.J. Calabrese, W.J. Kozumbo, The phytoprotective agent sulforaphane prevents inflammatory degenerative diseases and age-related pathologies via Nrf2-mediated hormesis, Pharmacol. Res. 163 (2021) 105283, https://doi.org/10.1016/j.phrs.2020.105283.

[23] L.-Y. Wei, et al., The functional role of sulforaphane in intestinal inflammation: a review, Food Funct. 13 (2) (2022) 514–529, https://doi.org/10.1039/d1fo03398k.

[24] H.-f. Gu, X.-y. Mao, M. Du, Metabolism, absorption, and anti-cancer effects of sulforaphane: an update, Crit. Rev. Food Sci. Nutr. 62 (13) (2022) 3437–3452, https://doi.org/10.1080/10408398.2020.1865871.

[25] X. Xu, et al., Effect of glucoraphanin from broccoli seeds on lipid levels and gut microbiota in high-fat diet-fed mice, J. Funct.Foods 68 (2020) 103858, https://doi.org/10.1016/j.jff.2020.103858.

[26] C.N. Armah, et al., A diet rich in high-glucoraphanin broccoli interacts with genotype to reduce discordance in plasma metabolite profiles by modulating mitochondrial function123, Am. J. Clin. Nutr. 98 (3) (2013) 712–722, https://doi.org/10.3945/ajcn.113.065235.

[27] L. Xu, N. Nagata, T. Ota, Glucoraphanin: a broccoli sprout extract that ameliorates obesity-induced inflammation and insulin resistance, Adipocyte 7 (3) (2018) 218–225, https://doi.org/10.1080/21623945.2018.1474669.

[28] N. Nagata, et al., Glucoraphanin ameliorates obesity and insulin resistance through adipose tissue browning and reduction of metabolic endotoxemia in mice, Diabetes 66 (5) (2017) 1222–1236, https://doi.org/10.2337/db16-0662.

[29] W. Zhu, et al., Robust UHPLC-(ESI+)-MS/MS method for simultaneous analysis of glucoraphanin, sulforaphane, and sulforaphane metabolites in biological samples, ACS Food Sci. Technol. 3 (7) (2023) 1300–1310, https://doi.org/10.1021/acsfoodscitech.3c00173.

[30] M. Da Silva, et al., Large procyanidins prevent bile-acid-induced oxidant production and membrane-initiated ERK1/2, p38, and Akt activation in Caco-2 cells, Free Radic. Biol. Med. 52 (1) (2012) 151–159, https://doi.org/10.1016/j.freeradbiomed.2011.10.436.

[31] X. Rao, et al., An improvement of the 2ˆ(-delta delta CT) method for quantitative real-time polymerase chain reaction data analysis, Biostat. Bioinforma. Biomath. 3 (3) (2013) 71–85. https://www.ncbi.nlm.nih.gov/pmc/articles/PMC4280562/.

[32] E. Daveri, et al., Hexameric procyanidins inhibit colorectal cancer cell growth through both redox and non-redox regulation of the epidermal growth factor signaling pathway, Redox Biol. 38 (2021) 101830, https://doi.org/10.1016/j.redox.2020.101830.

[33] J. Jumper, et al., Highly accurate protein structure prediction with AlphaFold, Nature 596 (7873) (2021) 583–589, https://doi.org/10.1038/s41586-021-03819-2.

[34] Y. Liu, et al., CB-Dock2: improved protein-ligand blind docking by integrating cavity detection, docking and homologous template fitting, Nucleic Acids Res. 50 (W1) (2022) W159–W164, https://doi.org/10.1093/nar/gkac394.

[35] R.M. Bheemreddy, E.H. Jeffery, The metabolic fate of purified glucoraphanin in F344 rats, J. Agric. Food Chem. 55 (8) (2007) 2861–2866, https://doi.org/10.1021/jf0633544.

[36] A.R. Cross, A.W. Segal, The NADPH oxidase of professional phagocytes—prototype of the NOX electron transport chain systems, BBA-Bioenergetics 1657 (1) (2004) 1–22, https://doi.org/10.1016/j.bbabio.2004.03.008.

[37] G. Aviello, U.G. Knaus, NADPH oxidases and ROS signaling in the gastrointestinal tract, Mucosal Immunol. 11 (4) (2018) 1011–1023, https://doi.org/10.1038/s41385-018-0021-8.

[38] R.A. El Hassani, et al., Dual oxidase2 is expressed all along the digestive tract, Am. J. Physiol. Gastrointest. Liver Physiol. 288 (5) (2005) G933–G942, https://doi.org/10.1152/ajpgi.00198.2004.

[39] R. Al-Sadi, et al., TNF-α modulation of intestinal epithelial tight junction barrier is regulated by ERK1/2 activation of Elk-1, Am. J. Pathol. 183 (6) (2013) 1871–1884, https://doi.org/10.1016/j.ajpath.2013.09.001.

[40] K.E. Cunningham, J.R. Turner, Myosin light chain kinase: pulling the strings of epithelial tight junction function, Ann. N. Y. Acad. Sci. 1258 (1) (2012) 34–42, https://doi.org/10.1111/j.1749-6632.2012.06526.x.

[41] K. Khoshbin, M. Camilleri, Effects of dietary components on intestinal permeability in health and disease, Am. J. Physiol. Gastrointest. Liver Physiol. 319 (5) (2020) G589–G608, https://doi.org/10.1152/ajpgi.00245.2020.

[42] A. Michielan, R.D. Incà, Intestinal permeability in inflammatory bowel disease: pathogenesis, clinical evaluation, and therapy of leaky gut, Mediat. Inflamm. (2015), https://doi.org/10.1155/2015/628157, 2015.

[43] L.J. John, M. Fromm, J.-D. Schulzke, Epithelial barriers in intestinal inflammation, Antioxidants Redox Signal. 15 (5) (2011) 1255–1270, https://doi.org/10.3389/fimmu.2023.1108289.

[44] Y.-S. Kim, et al., TNF-induced activation of the Nox1 NADPH oxidase and its role in the induction of necrotic cell death, Mol. Cell 26 (5) (2007) 675–687, https://doi.org/10.1016/j.molcel.2007.04.021.

[45] D.E. Iglesias, et al., Curcumin mitigates TNFα-induced caco-2 cell monolayer permeabilization through modulation of NF-κB, ERK1/2, and JNK pathways, Mol. Nutr. Food Res. 66 (21) (2022) e2101033, https://doi.org/10.1002/mnfr.202101033.

[46] E. Cremonini, et al., Anthocyanins protect the gastrointestinal tract from high fat diet-induced alterations in redox signaling, barrier integrity and dysbiosis, Redox Biol. 26 (2019) 101269, https://doi.org/10.1016/j.redox.2019.101269.

[47] E. Cremonini, et al., (-)-Epicatechin protects the intestinal barrier from high fat diet-induced permeabilization: implications for steatosis and insulin resistance, Redox Biol. 14 (2018) 588–599, https://doi.org/10.1016/j.redox.2017.11.002.

[48] W. Zhu, L. Xiong, P.I. Oteiza, Structure-dependent capacity of procyanidin dimers to inhibit inflammation-induced barrier dysfunction in a cell model of intestinal epithelium, Redox Biol. 75 (2024) 103275, https://doi.org/10.1016/j.redox.2024.103275.

[49] J. Bradley, TNF-mediated inflammatory disease, J. Pathol. 214 (2) (2008) 149–160, https://doi.org/10.1002/path.2287.

[50] T.Y. Ma, et al., TNF-α-induced increase in intestinal epithelial tight junction permeability requires NF-κB activation, Am. J. Physiol. Gastrointest. Liver Physiol. 286 (3) (2004) G367–G376, https://doi.org/10.1152/ajpgi.00173.2003.

[51] S.K. Moon, B.Y. Cha, C.H. Kim, ERK1/2 mediates TNF-α-induced matrix metalloproteinase-9 expression in human vascular smooth muscle cells via the regulation of NF-κB and AP-1: involvement of the ras dependent pathway, J. Cell. Physiol. 198 (3) (2004) 417–427, https://doi.org/10.1002/jcp.10435.

[52] D. Ye, T.Y. Ma, Cellular and molecular mechanisms that mediate basal and tumour necrosis factor-α-induced regulation of myosin light chain kinase gene activity, J. Cell Mol. Med. 12 (4) (2008) 1331–1346, https://doi.org/10.1111/j.1582-4934.2008.00302.x.

[53] Y. Jin, A.T. Blikslager, The regulation of intestinal mucosal barrier by myosin light chain kinase/rho kinases, Int. J. Mol. Sci. 21 (10) (2020) 3550, https://doi.org/10.3390/ijms21103550.

[54] E. Ihara, et al., ERK and p38 MAPK pathways regulate myosin light chain phosphatase and contribute to Ca2+ sensitization of intestinal smooth muscle contraction, Neuro Gastroenterol. Motil. 27 (1) (2015) 135–146, https://doi.org/10.1111/nmo.12491.

[55] D. Xiao, L.D. Longo, L. Zhang, α1-Adrenoceptor-mediated phosphorylation of MYPT-1 and CPI-17 in the uterine artery: role of ERK/PKC, Am. J. Physiol. Heart Circ. Physiol. 288 (6) (2005) H2828–H2835, https://doi.org/10.1152/ajpheart.01189.2004.

[56] P.P. Tak, G.S. Firestein, NF-κB: a key role in inflammatory diseases, J. Clin. Invest. 107 (1) (2001) 7–11, https://doi.org/10.1172/JCI11830.

[57] E.H. Jeffery, M. Araya, Physiological effects of broccoli consumption, Phytochemistry Rev. 8 (1) (2009) 283–298, https://doi.org/10.1007/s11101-008-9106-4.

[58] J.W. Fahey, et al., Sulforaphane bioavailability from glucoraphanin-rich broccoli: control by active endogenous myrosinase, PLoS One 10 (11) (2015) e0140963, https://doi.org/10.1371/journal.pone.0140963.

[59] R.-H. Lai, M.J. Miller, E. Jeffery, Glucoraphanin hydrolysis by microbiota in the rat cecum results in sulforaphane absorption, Food Funct. 1 (2) (2010) 161–166, https://doi.org/10.1039/c0fo00110d.

[60] S. Tian, et al., Microbiota: a mediator to transform glucosinolate precursors in cruciferous vegetables to the active isothiocyanates, J. Sci. Food Agric. 98 (4) (2018) 1255–1260, https://doi.org/10.1002/jsfa.8654.

[61] Y. He, et al., Effects of dietary fiber on human health, Food Sci. Hum. Wellness 11 (1) (2022) 1–10, https://doi.org/10.1016/j.fshw.2021.07.001.
[62] K. Ou, L. Gu, Absorption and metabolism of proanthocyanidins, J. Funct.Foods 7 (2014) 43–53, https://doi.org/10.1016/j.jff.2013.08.004.
[63] P.D. Cani, et al., Metabolic endotoxemia initiates obesity and insulin resistance, Diabetes 56 (7) (2007) 1761–1772, https://doi.org/10.2337/db06-1491.
[64] C.N. Armah, et al., Diet rich in high glucoraphanin broccoli reduces plasma LDL cholesterol: evidence from randomised controlled trials, Mol. Nutr. Food Res. 59 (5) (2015) 918–926, https://doi.org/10.1002/mnfr.201400863.